Evidence for the Formation of a Large-Scale Current Sheet in a Solar Flare

Linhui Sui[1] and Gordon D. Holman

Laboratory for Astronomy and Solar Physics, Code 682, NASA's Goddard Space Flight Center, Greenbelt, MD 20771

ABSTRACT

We present X-ray evidence for the formation of a large-scale current sheet in a flare observed by the Ramaty High Energy Solar Spectroscopic Imager on 2002 April 15. The flare occurred on the northwest limb, showing a cusp-shaped flare loop in the rise phase. When the impulsive rise in hard X-rays (> 25 keV) began, the cusp part of the coronal source separated from the underlying flare loop and remained stationary for about 2 minutes. During this time the underlying flare loops shrank at ~ 9 km s^{-1}. The temperature of the underlying loops increased towards higher altitudes, while the temperature of the coronal source increased towards lower altitudes. These results indicate that a current sheet formed between the top of the flare loops and the coronal source during the early impulsive phase. After the hard X-ray peak, the flare loops grew outward at ~ 8 km s^{-1}, and the coronal source moved outward at ~ 300 km s^{-1}, indicating an upward expansion of the current sheet. About 30 minutes later, post-flare loops seen in the SOHO Extreme Ultraviolet Imaging Telescope 195 Å passband rose at ~ 10 km s^{-1}. A large coronal loop-like structure, observed by the SOHO Large Angle and Spectrometric Coronagraph C2 and C3 detectors, also propagated outward at ~ 300 km s^{-1}. These observations are all consistent with the continued expansion of the current sheet.

Subject headings: Sun: flares—Sun: X-rays

1. Introduction

Magnetic reconnection is thought to play a fundamental role in solar flares. In the classical reconnection model (Carmichael 1964; Sturrock 1966; Hirayama 1974; Kopp & Pneuman

[1]Department of Physics, The Catholic University of America, 620 Michigan Ave, Washington, DC 20064.

1976), oppositely directed magnetic field lines are stretched to form a current sheet where they reconnect. The released magnetic energy is quickly converted to the thermal and kinetic energies of plasma and particles. The reconnected field lines retract downward to form post-flare loops, and upward to form a coronal plasmoid, and possibly a Coronal Mass Ejection (CME). Due to the upward propagation of the reconnection site, the post-flare loop system appears to rise. Decades of observations have provided many indirect pieces of evidence for this reconnection scenario: cusp-shaped soft X-ray flare loops (Tsuneta et al. 1992; Tsuneta 1996), increase of loop height and footpoint separation with time (Tsuneta et al. 1992), high temperature plasma along the field lines mapping to the tip of the cusp (Tsuneta 1996), a hard X-ray source located above the soft X-ray loops (Masuda et al. 1994), horizontal inflow above the cusp region (Yokoyama et al. 2001), downflow above the cusp-shaped loops (McKenzie & Hudson 1999), and an upward ejected plasmoid above the loops (Shibata et al. 1995; Ohyama & Shibata 1998).

Despite this evidence, we lack direct observations of the formation and evolution of a current sheet in a flare. As summarized by Ko et al. (2003), the high electrical conductivity and nearly force-free environment in the corona confine the current sheet to a very thin region in the tenuous corona, making it difficult to observe. Lin & Forbes (2000) and Lin (2002) claimed a current sheet develops following the onset of the eruption. Because the current sheet cannot be rapidly dissipated by magnetic reconnection, it can exist for a few hours or even a few days. There is some further observational evidence for current sheets associated with CMEs (Webb et al. 2001; Ciaravella et al. 2002; Ko et al. 2003).

In this Letter, we present evidence for the formation of a large-scale current sheet in a flare observed by the Ramaty High Energy Solar Spectroscopic Imager (RHESSI Lin et al. 2002). The flare occurred on the northwest limb in NOAA Active Region 9011 on 2002 April 15. It was classified as a GOES M1.2 flare. According to the SOHO Large Angle and Spectrometric Coronagraph (LASCO) CME catalog (*http://cdaw.gsfc.nasa.gov*), no CME was associated with this event, but a large, expanding coronal loop was observed with the LASCO C2 and C3 detectors.

2. Observations

RHESSI X-ray lightcurves in three energy bands are shown in Figure 1 (*top panel*). The RHESSI thin attenuators (Smith et al. 2002) were in throughout the flare observation, thus limiting the lower energy of the X-ray observations to $\sim$ 6 keV. The impulsive rise of hard X-rays (25-50 keV) started at 23:09:40 UT, and peaked around 23:11:30 UT.

During the rise phase of the flare (before 23:09:40 UT), the spatially integrated X-ray spectrum can be fitted with an isothermal bremsstrahlung function (exponential form) with a temperature of 20–30 MK. The RHESSI images obtained with the CLEAN imaging algorithm (Hurford et al. 2002) show a cusp-shaped flare loop. A 10-25 keV CLEAN image at 23:09:20 UT, just before the impulsive rise, is shown in Figure 2 (*left panel*). The cusp has a round tip, which is different from the cusp features often seen with the Yohkoh Soft X-ray Telescope (SXT) (Tsuneta et al. 1992; Tsuneta 1996), and the flare loop is not symmetric. More detailed analysis reveals that there are two loops involved in this flare: a large symmetric loop and a very small loop close to the northern footpoint of the larger loop. The detailed flare morphology is beyond the focus of this paper. A more comprehensive paper on this event with multi-wavelength analysis is in preparation. This paper focuses on the large, symmetric loop.

After the impulsive rise, the spatially integrated X-ray spectrum can be fitted with an isothermal bremsstrahlung function (T $\sim$ 30 MK) plus a single power-law component above 25 keV. Images in the 10-25 keV band at 23:09:40 and 23:10:00 UT are shown in Figure 2 (*middle and right panels*). The coronal source is separated from the flare loop. The coronal source stays stationary for about 2 minutes without obvious motion until after the peak of the flare. After the peak, the coronal source moves outward. Figure 3 shows a sequence of 10-25 keV images after the peak. An estimate of the speed, obtained using the centroid of the coronal source in each image, is 300 km s^{-1}.

RHESSI images in several narrow energy bands were obtained in 20-s time intervals throughout the flare. The energy widths $\Delta\epsilon$ were selected to ensure acceptable image quality: $\Delta\epsilon = 2$ keV within the range 4 keV $\leq \epsilon \leq$ 16 keV, 4 keV at 16 keV, 5 keV at 20 keV and 25 keV. The flare loops in the images have a very bright loop top. Therefore, the centroids of the loop top sources can represent the tops of the loops. Since the flare loop is symmetric, the height of the loop is defined as the distance between the centroid of the loop top and the center of the line between the two footpoints. Because the flare occurred very close to the limb (heliocentric longitude $\sim 80^\circ$), the projection effect is very small. Therefore, we neglect it in the loop height calculations.

Time histories of the loop height and coronal source height are shown in Figure 1 (*middle panel*). Because the thin attenuators substantially diminish the photon flux below 10 keV, we find that the images at 10-12 keV are the best to show the evolution of the loop height, and at 10-25 keV for the weaker coronal source. However, we do find that the time histories in other energy bands show a similar trend. Because of poor quality, images before 23:08:40 UT were not included in the study. As seen in the plot, the height of the loops decreases at the rise phase and the early impulsive phase, while the height of the coronal source remains

about the same. Soon after the peak of the flare the loops start to grow upward, and the coronal source starts moving outward at ~ 300 km s^{-1}. Linear fits indicate that the speed of the loop shrinkage, a term coined by Švestka et al. (1987), is 9 km s^{-1}, and the loop growth speed is about 8 km s^{-1}. The shrinkage speed obtained here is faster than that of Hiei & Hundhausen (1996), who obtained about 1 to 2 km s^{-1}. During this phase, the loops shrink by $\sim 20\%$ of their initial height. The loop growth speed is about the same as the rise speed of the inner loop top and the footpoint separation speed obtained by Tsuneta et al. (1992) with SXT, and the rise speed of the coronal source associated with an arcade of loops in the 2002 April 21 flare observed by RHESSI (Gallagher et al. 2002). About 30 minutes later, post-flare loops seen in the Extreme Ultraviolet Imaging Telescope (EIT) 195 Å passband rose at ~ 10 km s^{-1}.

Figure 1 (*bottom panel*) shows the height of the flare loops and the coronal source in different energies at 23:11:00 UT, a time immediately before the hard X-ray peak. Because of the poor quality, the image in the 4-6 keV band was not included in the plot. We find that the loop height increases with energy, indicating cooler loops nest under hotter loops. This agrees with the SXT and recent RHESSI observational results (Tsuneta et al. 1992; Tsuneta 1996; Gallagher et al. 2002). The apparent sudden increase of the loop height around 17 keV is probably due to the displacement of the Masuda-type hard X-ray coronal source from the thermal flare loops (Nitta et al. 2001). On the other hand, we find that the altitude of the coronal source decreases with energy, implying the temperature of the coronal source increases downward. Thus, the temperature variation of the coronal source with source altitude is the opposite to that of underlying loops. The temperature variation with source altitude is shown in Figure 4, where both the loops and the coronal source are shown in different energy bands at 23:11:00 UT.

3. Discussion and Conclusions

We believe the observational results presented above provide clear evidence for current sheet formation in the flare. The main arguments are the following: (1) the temperature distribution pattern of the flare loops and the coronal source in the early impulsive phase indicates that a current sheet is formed between the top of the flare loops and the coronal source. The temperature distribution of the loops is interpreted in terms of energy supply by reconnection near the top of the loop and the subsequent cooling of the inner loops by heat conduction and filling with evaporated plasma from the chromosphere (Švestka et al. 1987). Above the current sheet, the plasma close to the sheet will also be heated by the energy supplied from the reconnection. Due to adiabatic cooling and conduction, the cooler

sources are located further above the current sheet. (2) The sudden change in images (Fig. 2) indicates the magnetic field configuration changed from X-type to Y-type during the current sheet formation. The magnetic field configuration is X-type before the impulsive rise. An X-type neutral point tends to be locally unstable, provided the sources of the field are free to move (Dungey 1953). After the impulsive rise the X-type magnetic configuration collapses to a configuration with a current sheet having Y-points at its ends (Priest & Forbes 2000). The mechanism of the collapse is still unclear. The length of the current sheet before the hard X-rays peak, i.e. the distance between the top of the loops and the coronal source, is $\sim 1.2\times10^4$ km. (3) The loop shrinkage before the hard X-ray peak is most likely caused by the change of the magnetic field configuration as the X-point collapsed into a current sheet. The loop shrinkage observed here is different from the shrinkage discussed by Švestka et al. (1987), Lin et al. (1995), and Forbes & Acton (1996). The shrinkage they have studied is for individual lines or loops, and is due to either the reconnected loop retracting from the current sheet or the cooling of hotter loops. We believe that the shrinkage here might be caused by the change of field configuration during the current sheet formation. An alternative explanation for the shrinkage is that the flare loops move eastward along an arcade. However, checking the time history of the centroids of the footpoints, we do not find a systematic footpoint motion. Therefore, we conclude that motion of the entire loop system cannot explain this shrinkage.

The observation of growing loops, indicating upward motion of the lower tip of the current sheet, is consistent with the classical model. The model predicts that the magnetic field lines are first opened up to form a vertical current sheet, and then magnetic field lines in the current sheet successively reconnect to form growing flare loops. The 8 km s^{-1} growth speed in this flare agrees with the speeds obtained with Yohkoh SXT. Moreover, we observed a coronal source moving outward at $\sim$ 300 km s^{-1} after the hard X-ray peak, which we interpret as the upper tip of the current sheet. Forbes & Priest (1995) have developed a force-free model of an eruptive flare or CME which is triggered by an erupting coronal flux rope. A vertical current sheet is created below the flux rope. Lin & Forbes (2000) and Lin (2002) investigated the behavior of the current sheet in the eruptive process with a two-dimensional flux-rope model. They found that both the lower tip and the upper tip of the current sheet move upward when magnetic reconnection occurs, and the upper tip moves faster than the lower tip by $\sim$ 200-700 km s^{-1}, in agreement with our observations.

If we assume the coronal source moved outward at a constant speed, i.e. 300 km s^{-1}, then it exited the field of view of our RHESSI image around 23:14:00 UT. However, we find some weaker coronal sources along the expanded current sheet at later times in the RHESSI images. These sources are possibly caused by the tearing-mode resistive instability in the current sheet (Furth et al. 1963). We also estimated the location of the moving coronal

source at 02:26:00 UT on 2002 April 16 when the large coronal loop was first seen in the LASCO C2 image. Interestingly, we find that at that time the RHESSI coronal source would have reached the inner edge of the coronal loop in the LASCO C2 image. We also find that the large coronal loop propagates outward up to 16 $R_{\odot}$ at a constant speed of $\sim$ 300 km s^{-1}. Therefore, we think the outward moving source observed in this flare is part of an upward ejected plasmoid (or a large-scale helically twisted loop), such as has been reported by Shibata et al. (1995) and Ohyama & Shibata (1998) using Yohkoh SXT. This also supports the idea that the hot plasma ejections might be miniature versions of the much larger CME events (Shibata et al. 1995).

Based on our observational results, it is interesting to speculate on the timing of the current sheet formation and flare energy release rate. In the rise phase of the flare, the current sheet has not yet formed, and the magnetic field configuration is X-type. The reconnection rate is slow, and most of the released magnetic energy heats the plasma within the loops near the neutral point, so the RHESSI images only show thermal flare loops. In the impulsive phase, the current sheet forms and the field configuration becomes Y-type. The reconnection rate suddenly increases. The appearance of the flare loop footpoints in the hard X-ray images (25-50 keV) indicates that nonthermal particles are accelerated and dumped into the solar lower atmosphere. Therefore, the magnetic energy dissipated by the reconnection goes both to heating the plasma and accelerating particles. Perhaps this impulsive phase is associated with faster Petschek-type reconnection. After the peak of the hard X-ray emission the current sheet stretches into a Sweet-Parker type of configuration. The energy release rate decreases as the current sheet expands.

We are grateful to Jun Lin and Brian Dennis for valuable discussions and comments on the manuscript, and to Kim Tolbert, Dominic Zarro, and Peter Gallagher for their help with software. We also thank the referee, John Raymond, for valuable comments on the paper. The work is supported by the NASA Sun-Earth Connection Program and the RHESSI project.

REFERENCES

Carmichael, H. 1964, In The Physics of Solar Flares, ed. W. N. Hess (NASA SP-50, Washington, DC:NASA), 451

Ciaravella, A., Raymond, J.C., Li, J., Reiser, P., Gardner, L.D., Ko, Y.-K., & Fineschi, S. 2002, ApJ, 575, 1116

Dungey, J.W. 1953, Conditions for the occurrence of electrical discharges in astrophysical systems, Phil. Mag., 44, 725

Forbes, T.G., & Priest, E.R. 1995, ApJ, 446, 377

Forbes, T.G., & Acton, T.W. 1996, ApJ, 459, 330

Furth, H.P., Killeen, J., & Rosenbluth, M.N. 1963 Finite-resistivity instablitities of a sheet pinch, Phys. Fluids, 6, 459

Gallagher, P.T., Dennis, B.R., Krucker, S., Schwartz, R.A., & Tolbert, A.K. 2002, Sol. Phys., 210, 341

Hiei, E., & Hundhausen, A. 1996, in Magnetodynamic Phenomena in the Solar Atmosphere, Ed. Y. Uchida, T. Kosugi, & H. Hudson (Kluwer, Tokyo), 125

Hirayama, T. 1974, Sol. Phys., 34, 323

Hurford, G.J., et al. 2002, Sol. Phys., 210, 61

Ko, Y.-K., Raymond, J.C, Lin, J., Lawrence G., Li, J., Fludra, A. 2003, ApJ, 594, 1068

Kopp, R.A., & Pneuman, G.W. 1976, Sol. Phys., 50, 85

Lin, R.P., et al. 2002, Sol. Phys., 210, 3

Lin, J., Forbes, T.G., Priest, E. R., & Bungey, T.N. 1995, Sol. Phys., 159, 275

Lin, J., & Forbes, T.G. 2000, J. Geophys. Res., 105, 2375

Lin, J. 2002, Chinese J. Astron. Astrophys., 2, 539

Masuda, S., Kosugi, T., Hara, H., Tsuneta, S., & Ogawara, Y. 1994, Nature, 371, 495

McKenzie, D.E., & Hudson, H.S. 1999, ApJ, 519, 93

Nitta, N. V., Sato, J., Hudson, H.S. 2001, ApJ, 552, 821

Ohyama, M., & Shibata, K. 1998 ApJ, 499, 934

Priest, E., & Forbes, T. 2000, Magnetic Reconntion, MHD Theory and Applications, Cambridge University Press

Shibata, K., Masuda, S., Shimojo, M., Hara, H., Yokoyama, T., Tsuneta, S., Kosugi, T., & Ogawara, Y. 1995, ApJ, 451, 83

Smith, D.M., et al. 2002, Sol. Phys., 210, 33

Švestka, Z., Fontenla, J.M., Machado, M.E., Martin, S.T., Neidig, D.F. and Poletto, G. 1987, Sol. Phys., 108, 237

Sturrock, P.A., 1966, Nature, 211, 695

Tsuneta, S., Hara, H., Shimizu, T., Acton, L.W., Strong, K.T., Hudson, H.S., & Ogawara, Y. 1992, PASJ, 44, 63

Tsuneta, S. 1996, ApJ, 456, 840

Tsuneta, S. 1997, ApJ, 483, 507

Webb, D.F., Burkepile, J., Forbes, T.G., & Riley P. 2003, J. Geophys. Res., in press

Yokoyama T., Akita, K., Morimoto, T., Inoue, K., Newmark, J. 2001, ApJ, 546, 69

This preprint was prepared with the AAS LaTeX macros v5.0.

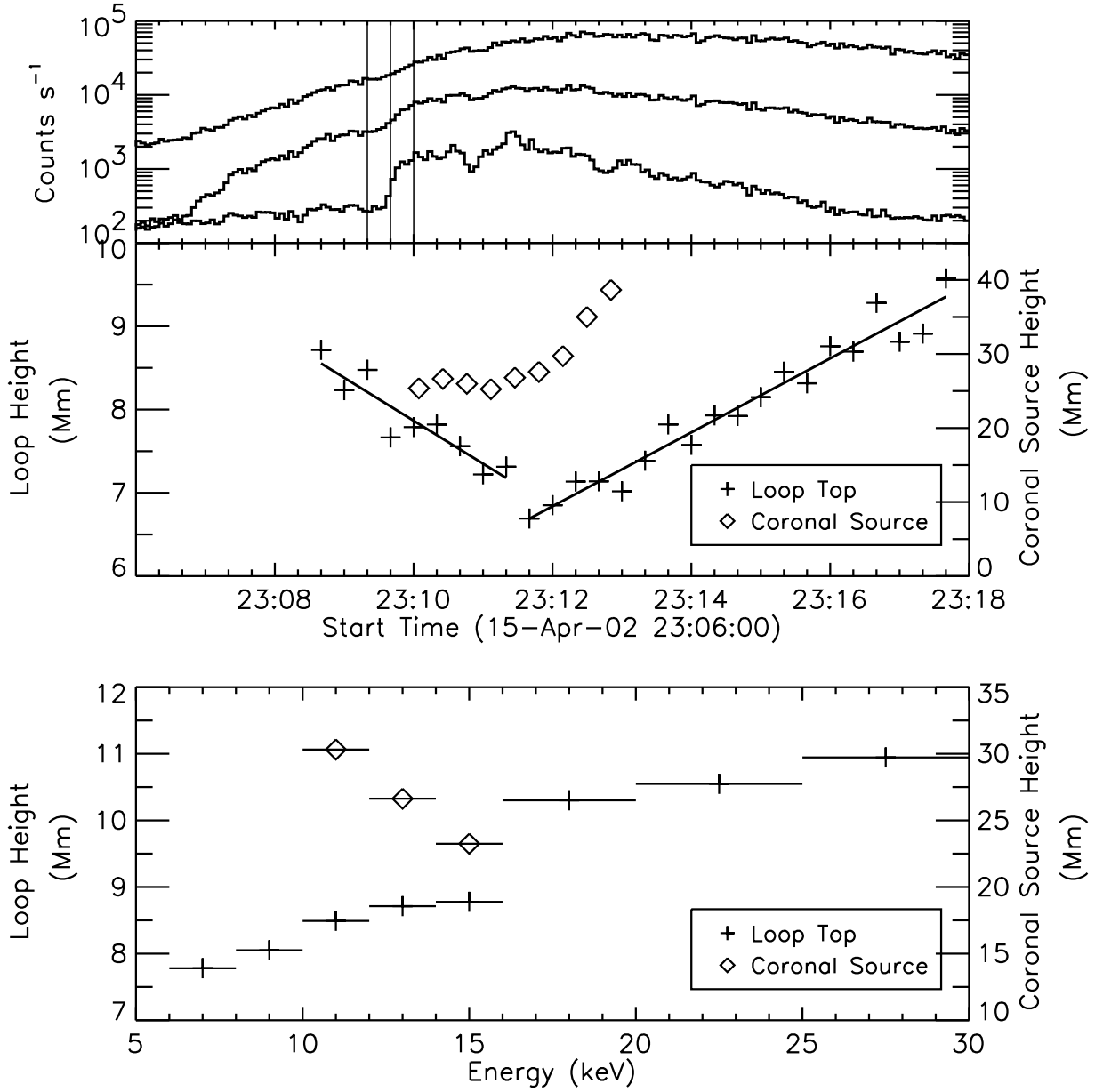

Fig. 1.— *Top panel*: RHESSI light curves in three energy bands (from top to bottom): 3-12 keV, 12-25 keV, 25-50 keV. To avoid overlap, the light curves are scaled by 2.0, 0.5, and 1.0, respectively. The three vertical lines mark the start time of each image in Figure 2. *Middle panel*: time histories of loop height (obtained from 10-12 keV images) and coronal source height (obtained from 10-25 keV images). The solid lines are the linear fits. *Bottom panel*: the height of the loop and the coronal source at different energies at 23:11:00 UT. The horizontal bars represent the energy bandwidth of the RHESSI images.

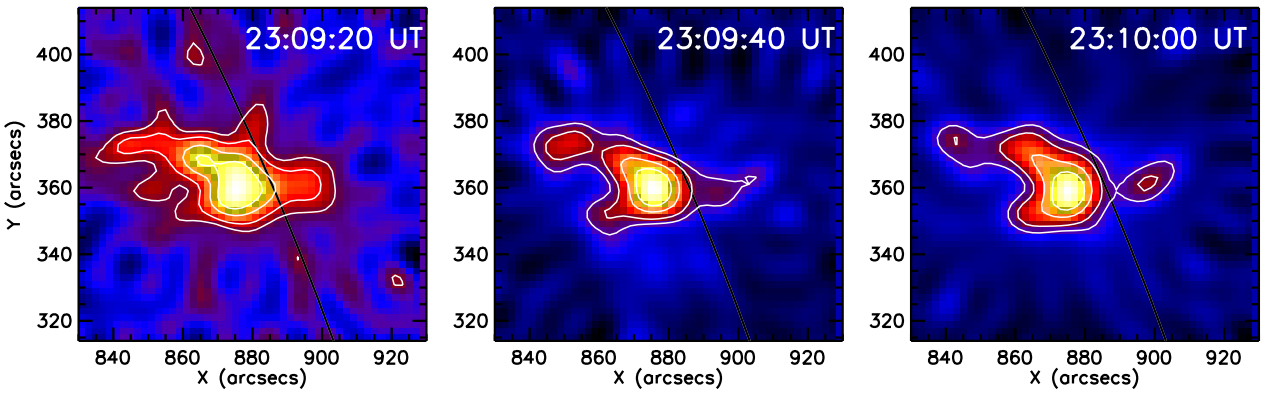

Fig. 2.— RHESSI 10-25 keV images at 23:09:20 UT (just before the impulsive rise), 23:09:40 UT and 23:10:00 UT (just after the impulsive rise). The integration time for each image is 20 s. RHESSI grids 3-9 were used, giving an angular resolution $\sim 7''$. The contour levels (normalized to the peak flux of each image) are 0.2, 0.3, 0.5, and 0.7.

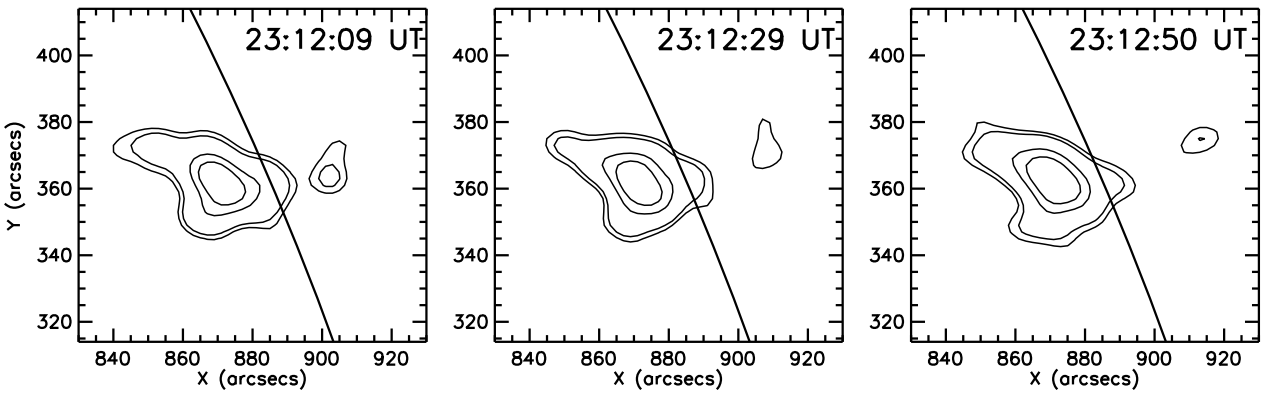

Fig. 3.— A time sequence of 10-25 keV RHESSI images after the hard X-ray peak. The integration time of each image is 20.75 s (5 rotations). RHESSI grids 3-9 were used, giving an angular resolution $\sim 7''$. The contour levels (normalized to the peak flux of each image) are 0.15, 0.2, 0.5, and 0.7.

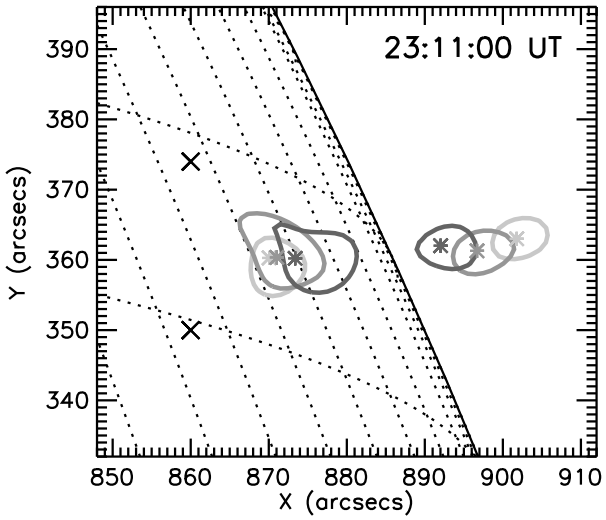

Fig. 4.— RHESSI images in different energy bands at 23:11:00 UT. The three contours (80% of the peak flux in each image) on the solar disk indicate the top of loops in the energy bands (contour line shade from light to dark): 6-8 keV, 10-12 keV, and 16-20 keV. The contours (80% of the peak flux of the coronal source in each image) above the limb are for the (from light to dark) 10-12 keV, 12-14 keV, and 14-16 keV bands. The '$*$' marks the centroid of each source. The '$\times$' signs mark the two footpoints of the X-ray loop.